2014

Phase composition and nanostructure of Zr_2Co_{11}-based alloys

Y.L. Jin
University of Nebraska-Lincoln, yjin4@unl.edu

Wenyong Zhang
University of Nebraska-Lincoln, wenyong.zhang@unl.edu

Ralph A. Skomski
University of Nebraska-Lincoln, rskomski2@unl.edu

Shah R. Valloppilly
University of Nebraska-Lincoln, svalloppilly2@unl.edu

Jeffrey E. Shield
University of Nebraska-Lincoln, jshield@unl.edu

See next page for additional authors

JOURNAL OF APPLIED PHYSICS **115**, 17A739 (2014)

Phase composition and nanostructure of Zr_2Co_{11}-based alloys

Y. L. Jin,[1,2] W. Y. Zhang,[1,2] R. Skomski,[1,2] S. Valloppilly,[1] J. E. Shield,[1,3] and D. J. Sellmyer[1,2,a)]

[1]*Nebraska Center for Materials and Nanoscience, University of Nebraska, Lincoln, Nebraska 68588, USA*
[2]*Department of Physics and Astronomy, University of Nebraska, Lincoln, Nebraska 68588, USA*
[3]*Department of Mechanical and Materials Engineering, University of Nebraska, Lincoln, Nebraska 68588, USA*

(Presented 6 November 2013; received 23 September 2013; accepted 26 November 2013; published online 3 March 2014)

The effect of Mo addition on phase composition and nanostructure of nanocrystalline $Zr_{16}Co_{84-x}Mo_x$ ($x = 0$–2.0) melt spun at 55 m/s has been investigated. All the ribbons consist mainly of a hard magnetic Zr_2Co_{11} phase with rhombohedral crystal structure but also contain minor amounts of soft-magnetic phases. The increase in cell volume on alloying suggests that Mo mainly enters the rhombohedral Zr_2Co_{11} structure and occupies the Co site. Mo addition promotes the formation of the hard magnetic phase and increases its volume fraction. The mean grain size of the hard magnetic phase remains almost unchanged with the increase of Mo content. But the average grain size of the soft magnetic phase decreases from about 200 nm to 50 nm. This promotes the exchange coupling of the hard and soft magnetic phases and thus leads to a significant increase in coercivity and isotropic energy product, from 0.6 kOe and 0.5 MGOe for $x = 0$ to 2.9 kOe and 4.2 MGOe for $x = 1.5$. © *2014 AIP Publishing LLC*. [http://dx.doi.org/10.1063/1.4867226]

INTRODUCTION

Zr_2Co_{11} is a good candidate for the development of permanent magnets without rare earth and noble metals, since it exhibits good intrinsic properties.[1–3] Depending on the preparation process, the crystal structure of Zr_2Co_{11} may be rhombohedral or orthorhombic.[4–6] Among these phases, rhombohedral Zr_2Co_{11} has been demonstrated to be the hard magnetic phase,[7] and a high quenching rate favors the formation of the hard magnetic phase.[8] Recently, an impressive energy product comparable to that of sintered $SmCo_5$ was obtained for the easy-axis aligned Zr_2Co_{11}-based nanocomposites produced by a single step cluster-deposition method.[9] However, its coercivity ($H_c \ll J_s/2$) is too small to further improve magnetic properties. Element addition is a feasible way to modify nanostructure and enhance coercivity. Much work has been done on increasing the coercivity and improving the rectangularity of the demagnetization curve for Zr-Co alloys by adding elements such as B, Ti, and Zr.[10–13] A very high coercivity for Zr-Co alloys, close to that of melt-spun $Nd_2Fe_{14}B$, has been achieved due to Mo addition and annealing.[14] However, it has been unclear so far how Mo additions affect the phase composition and nanostructure of nanocrystalline Zr_2Co_{11}-based alloys.

In this study, nanocrystalline $Zr_{16}Co_{84-x}Mo_x$ ($x = 0$, 0.5, 1.0, 1.5, and 2.0) has been prepared by melt spinning. $Zr_{16}Co_{84}$ corresponds to a Co:Zr ratio of 10.5:2, and a high wheel speed of 55 m/s was chosen in order to obtain a large volume fraction of the hard-magnetic phase. We find that phase composition and nanostructure strongly depend on the Mo content. Proper Mo addition increases the volume fraction of the hard magnetic phase and decreases the mean grain size of the soft magnetic phases, helping to improve coercivity and energy product.

EXPERIMENTAL METHODS

Ingots of $Zr_{16}Co_{84-x}Mo_x$ ($x = 0$, 0.5, 1, 1.5, 2.0) were prepared by arc melting high-purity elements in an argon atmosphere. The ribbons, which are about 2 mm wide and 50 μm thick, were made by ejecting molten alloys in a quartz tube onto the surface of a copper wheel with a speed of 55 m/s. The phase components were examined by XRD, with a Rigaku D/Max-B x-ray diffractometer (XRD) and Co Kα radiation, and by thermomagnetic measurements using a physical property measurement system (PPMS) at temperatures up to 1000 K. The nanostructure was observed with a FEI Tecnai Osiris Transmission Electron Microscope (TEM). To measure the hysteresis loops in fields of up to 7 T, we have used a superconducting quantum interference device (SQUID). The law of approach to saturation was used to fit high-field part of M(H) curves and calculate saturation magnetization M_s, magnetocrystalline anisotropy field H_a. In all magnetic measurements, the external magnetic field was applied parallel to the long direction of the ribbon.

RESULTS AND DISCUSSION

Figures 1(a) and 1(b) show the XRD patterns of nanocrystalline $Zr_{16}Co_{84-x}Mo_x$($x = 0$, 1.5) and the enlarged part of diffraction peaks from 43° to 46°. The diffraction peaks of all the samples are identified as orthorhombic Zr_2Co_{11} and rhombohedral Zr_2Co_{11}, which is the hard magnetic phase. The increase in cell volume on alloying suggests that Mo mainly enters the rhombohedral Zr_2Co_{11} structure and occupies one of the Co sites. The relative intensity of the

a)Author to whom correspondence should be addressed. Electronic mail: dsellmyer@unl.edu.

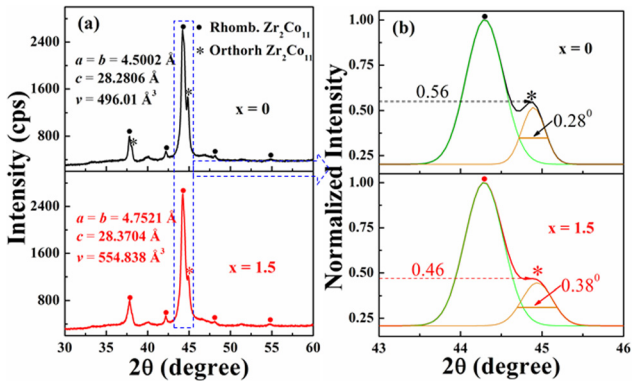

FIG. 1. XRD patterns of the nanocrystalline $Zr_{16}Co_{84-x}Mo_x$ ($x = 0$, 1.5) (a) and the enlarged part of diffraction peaks from 43° to 46° (b).

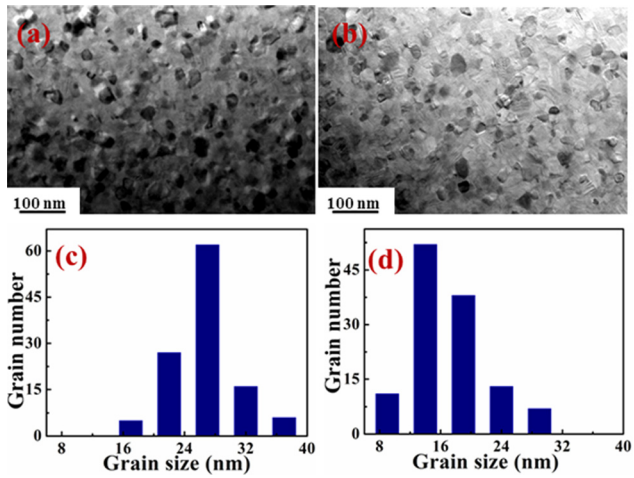

FIG. 3. TEM images of the nanocrystalline $Zr_{16}Co_{84-x}Mo_x$ (a) $x = 0$, (b) $x = 1.5$, and the statistical distribution of the grain size for (c) $x = 0$, (d) $x = 1.5$.

diffraction peaks of orthorhombic Zr_2Co_{11} for the $x = 1.5$ is lower than that for the $x = 0$, indicating that Mo addition restrains the formation of orthorhombic Zr_2Co_{11} and promotes the generation of the hard magnetic phase. We therefore conclude that Mo addition increases the volume fraction of the hard phase. The full width at half maximum (FWHM) of the peak at 44.3° for the $x = 1.5$ is almost the same as that for the $x = 0$, meaning that the average grain size of the hard magnetic phase remains almost unchanged with the increase of Mo content. The FWHM of the peak at 44.9° for the $x = 1.5$ is larger than that for the $x = 0$, indicating that the average grain size of the orthorhombic Zr_2Co_{11} decreases with x increasing.

Figure 2(a) shows the $M(T)$ curves of the nanocrystalline $Zr_{16}Co_{84-x}Mo_x$ ($x = 0$, 1.5) in a field of 1 kOe. Figure 2(b) presents the corresponding dM/dT curves in which the Curie temperatures (T_R and T_O) of the magnetic phases were determined. Two ferromagnetic-paramagnetic transitions were seen for the $x = 0$. They correspond to the orthorhombic and rhombohedral Zr_2Co_{11}. The second transition is harder to see for the $x = 1.5$, indicating that the Mo addition suppresses the formation of the orthorhombic Zr_2Co_{11} phase. This is in good agreement with the XRD results. The Curie temperature (T_R) of the rhombohedral Zr_2Co_{11} for the $x = 1.5$ is 720 K lower than that for the $x = 0$. This further demonstrates that Mo mainly enters the rhombohedral Zr_2Co_{11} and locates at the Co site. The magnetization at 948 K is not zero for the both samples. It indicates the existence of a small amount of Co which was not detected in the XRD patterns.

The TEM is a powerful tool to observe nanostructure such as grain size, shape, and distribution. Figures 3(a) and 3(b) show the TEM images of the nanocrystalline $Zr_{16}Co_{84-x}Mo_x$ ($x = 0$, 1.5). The maxtrix phase is supposed to be the rhombohedral Zr_2Co_{11}. The relatively small grains are believed to be the orthorhombic Zr_2Co_{11} and soft magnetic Co phases. Figures 3(c) and 3(d) show that the mean grain sizes of the soft phase for $x = 0$ and $x = 1.5$ are 30 nm and 15 nm, respectively. This reveals that the Mo addition refines the grain size of the soft phase, which matches with the XRD results.

Figure 4(a) shows the $M(H)$ curves of the nanocrystalline $Zr_{16}Co_{84-x}Mo_x$ ($x = 0$, 1.5, 2.0). It is evident that Mo addition improves the hysteresis-loop shape (rectangularity). Figure 4(b) presents the Mo-content dependence of spontaneous magnetization M_s, anisotropy field H_a, intrinsic coercivity, and energy product. As discussed above, Mo addition increases the volume fraction of the hard magnetic phase, refines the nanostructure, and promotes the interphase exchange coupling. Simultaneously, it leads to a small increases of H_a. Therefore, the coercivity increases with the increase in Mo content. This leads to a significant increase of energy product from 0.5 MGOe for $x = 0$ to 4.2 MGOe for $x = 1.5$. The best magnetic properties were obtained for the $x = 1.5$. Excessive Mo addition results in the appearance of amorphous phase which behaves as the nucleation site of reverse domain. This means that the coercivity reaches a maximum as function of x and then decreases. The critical grain size (R_c) for fully exchange coupling of soft phase equals to $2\pi\sqrt{A/2K}$, where A is the exchange constant of soft magnetic phase and K is magnetocrystalline anisotropy constant

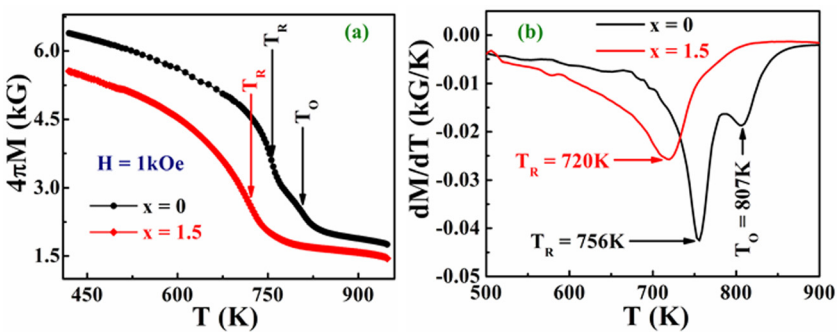

FIG. 2. $M(T)$ curves (a) of the nanocrystalline $Zr_{16}Co_{84-x}Mo_x$ ($x = 0$, 1.5) and corresponding dM/dT curves (b) from which the respective Curie temperatures T_R and T_O of the rhombohedral and orthorhombic phases are determined.

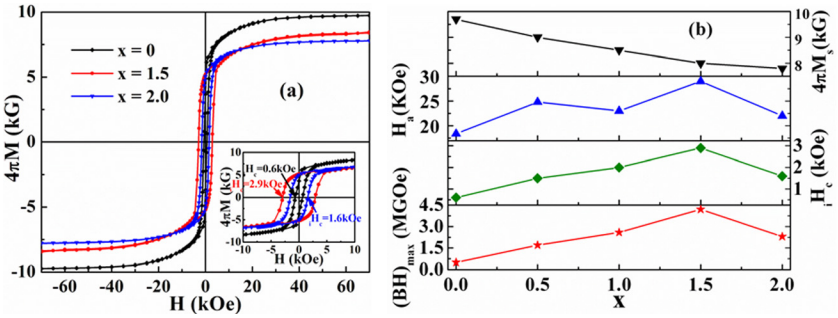

FIG. 4. Magnetic properties of nanocrystalline $Zr_{16}Co_{84-x}Mo_x$ ($x = 0$, 1.5, 2.0): (a) $M(H)$ curves and (b) spontaneous magnetization M_s, anisotropy field H_a, intrinsic coercivity ${}_iH_c$, and energy product $(BH)_{max}$.

of hard magnetic phase.[15] In this work, K for the rhombohedral Zr_2Co_{11} is about 10 Merg/cm^3. Generally, A is proportional to Curie temperature. A for the orthorhombic Zr_2Co_{11} and Co(Zr) is estimated to be 500 nerg/cm. So, $R_c = 10$ nm. For the $x = 1.5$ sample, the grain size of the soft phase is distributed in 9–29 nm (see Figure 3(d)). There are still many poorly exchange-coupled soft regions that switch easily. It is expected that coercivity and remanence will be further improved by adding B and narrowing the grain size distribution.

CONCLUSIONS

The molybdenum-content dependence of phase composition and nanostructure of nanocrystalline $Zr_{16}Co_{84-x}Mo_x$ ($x = 0$–2.0) produced by melt spinning has been studied. The ribbons consist mainly of the rhombohedral and orthorhombic Zr_2Co_{11} phases. Mo mainly enters the rhombohedral Zr_2Co_{11} structure and occupies the Co sites. Mo addition promotes the formation of the rhombohedral hard-magnetic phase and increases its volume fraction. The mean grain size of the hard magnetic phase remains almost unchanged with increasing Mo content, but the average grain size of the soft magnetic phase decreases from about 30 nm to 15 nm. This promotes the effective exchange coupling of the soft phases and thus leads to a significant increase in coercivity and energy product. The hard magnetic properties of the nanocrystalline $Zr_2(Co, Mo)_{11}$ may be further enhanced by grain alignment.

ACKNOWLEDGMENTS

This work was supported by Department of Energy/BREM (No. DE-AC02-07CH11358, Subaward No. SC-10-343). This research was performed in part in Central Facilities of the Nebraska Center for Materials and Nanoscience, which is supported by the Nebraska Research Initiative. Electron microscopy research was supported by NSF-MRI (DMR-0960110).

[1]T. Ishikawa and K. Ohmori, IEEE Trans. Magn. **26**, 1370 (1990).
[2]E. Burzo, R. Grössinger, P. Hundegger, H. R. Kirchmayr, R. Krewenka, and R. Lemaire, J. Appl. Phys. **70**, 6550 (1991).
[3]H. H. Stadelmaier, T. S. Tang, and E. -Th. Henig, Mater. Lett. **12**, 295 (1991).
[4]G. V. Ivanova, N. N. Shchegoleva, and A. M. Gabay, J. Alloys Compd. **432**, 135 (2007).
[5]B. G. Demczyk and S. F. Cheng, J. Appl. Crystallogr. **24**, 1023 (1991).
[6]A. M. Gabay, Y. Zhang, and G. C. Hajipanayis, J. Magn. Magn. Mater. **236**, 37 (2001).
[7]W. Y. Zhang, X. Z. Li, S. Valloppilly, R. Skomski, J. E. Shield, and D. J. Sellmyer, J. Phys. D: Appl. Phys. **46**, 135004 (2013).
[8]G. V. Ivanova and N. N. Shchegoleva, Phys. Met. Metallogr. **107**, 270 (2009).
[9]B. Balamurugan, B. Das, W. Y. Zhang, R. Skomski, and D. J. Sellmyer, Advanc. Mater. **25**, 6090 (2013).
[10]A. M. Gabai, N. N. Shchegoleva, V. S. Gaviko, and G. V. Ivanova, Phys. Metals Metallography **95**, 122 (2003).
[11]L. Y. Chen, H. W. Chang, C. H. Chiu, C. W. Chang, and W. C. Chang, J. Appl. Phys. **97**, 10F307 (2005).
[12]J. B. Zhang, Q. W. Sun, W. Q. Wang, and F. Su, J. Alloys Compd. **474**, 48 (2009).
[13]M. Y. Zhang, J. B. Zhang, C. J. Wu, W. Q. Wang, and F. Su, Physica B **405**, 1725 (2010).
[14]W. Y. Zhang, S. R. Valloppilly, X. Z. Li, R. Skomski, J. E. Shield, and D. J. Sellmyer, IEEE Trans. Magn. **48**, 3603 (2012).
[15]E. F. Kneller and R. Hawig, IEEE Trans. Magn. **27**, 3588 (1991).